Below we addressed the reviewer's comments carefully, with the reviewers' comments in black and our response in blue.

This manuscript presents a comprehensive investigation of aerosol hygroscopicity at a rural site in eastern China. By combining humidified light-scattering measurements, particle size distributions, and chemical composition with a Mie-theory-based inversion and ZSR closure approach, the authors provide a useful framework for constraining ambient κ_{OA} and investigating its controlling factors. The results provide interesting insights into the source-dependent response of OA hygroscopicity. The manuscript is generally well written, I have a few suggestions before the manuscript can be accepted for publication in ACP.

Response: We sincerely thank the reviewer for the positive and constructive assessment of our manuscript. We appreciate the reviewer's recognition of our methodology and findings. We have carefully considered all the comments and revised the manuscript accordingly. We believe these revisions have further improved the clarity and robustness of the manuscript. Our point-by-point responses are provided below.

1. Lines 270–274: OA hygroscopicity (κ_{OA}) is derived from κ_{inv} using the ZSR mixing rule and therefore depends on the retrieved κ_{inv}, the assumed hygroscopicity parameters, and the estimated volume fractions of the individual aerosol components. Uncertainties in these quantities may become particularly important when the residual term used to derive κ_{OA} is small. Please discuss the sensitivity of κ_{OA} to the major uncertainties and assumptions involved in Eq. (11).

Response: We thank the reviewer for this insightful comment. We agree that the uncertainty in κ_{OA} derived using the ZSR mixing rule (Eq. 11 in the manuscript) depends on the uncertainties in κ_{inv}, the assumed hygroscopicity parameters of the aerosol components, and their estimated volume fractions. In particular, when the OA volume fraction is small, uncertainties in the non-OA contributions can be amplified in the retrieved κ_{OA}.

To quantify the sensitivity of κ_{OA} to these uncertainties, we performed a Monte Carlo uncertainty propagation analysis with 10,000 realizations for each measurement point. The analysis accounted for uncertainties in κ_{inv}, the mass concentrations of non-refractory aerosol species measured by the ToF-ACSM, the total particle volume concentration (V_{PM}) derived from the particle number size distribution (PNSD), and the hygroscopicity parameter of refractory particulate matter other than BC (κ_{rPM}). The assumed uncertainties were based on those reported by Kuang et al. (2021), whose methodology for retrieving aerosol hygroscopicity is consistent with that used in this

study. For example, a relative uncertainty of 20% was assigned to the mass concentrations of all non-refractory species (including sulfate, nitrate, ammonium, chloride, and OA) measured by the ToF-ACSM. For κ_{rPM}, a baseline value of 0.05 and an absolute standard deviation of 0.03 were used to represent its uncertainty.

The Monte Carlo results show that the campaign-average κ_{OA} remains 0.11, consistent with the baseline estimate, and the Monte Carlo mean values are highly correlated with the baseline estimates (r = 0.99; Figure 2-1). However, the propagated standard deviations vary substantially among measurement points, ranging from 0.01 to 0.18. Larger uncertainties generally occur at higher κ_{OA} values and lower OA volume fractions (Figure 2-2), indicating enhanced sensitivity of the ZSR-based retrieval when the OA contribution to total particle volume is small. Additional sensitivity tests in which individual input parameters were perturbed separately further show that uncertainties in V_{PM} and κ_{rPM} contribute most strongly to the uncertainty in the retrieved κ_{OA}.

These results have been incorporated into the revised manuscript (Sections 2.3.3 and 3.2) to clarify the sensitivity of κ_{OA} to the major uncertainties and assumptions in Eq. (11). The corresponding results are also presented in Figures R2-1 and R2-2 in this response and Figure S15 and S16 in the Supplementary Information.

Section 2.3.3, lines 278-283: "***The derived κ_{OA} may be subject to uncertainties in the input parameters used in the inversion, thus, we performed a Monte Carlo uncertainty propagation analysis, with 10,000 realizations for each data point in the κ_{OA} time series. In each realization, the input variables in Eqs. 10 and 11 were randomly perturbed according to their prescribed uncertainties. Given the similarities in the measurement and inversion methods, the uncertainties assigned to the input variables, including the mass concentrations of non-refractory aerosol species measured by the ToF-ACSM, V_{PM}, κ_{inv} and κ_{rPM}, were based on the estimates reported in Table 2 of Kuang et al. (2021).***"

Section 3.3, lines 353-359: "***Monte Carlo uncertainty analysis showed that he standard deviations of the simulated κ_{OA} distributions at individual measurement points ranged from 0.01 to 0.18 (Fig. S15). Larger uncertainties generally occurred at higher κ_{OA} values and lower OA volume fractions, indicating greater sensitivity of the ZSR-based retrieval under these conditions (Fig. S16). Despite the substantial point-by-point uncertainties, the Monte Carlo mean values agreed well with the baseline estimates (Fig. S15a), yielding the same campaign-average κ_{OA} of 0.11 and a correlation coefficient of 0.99 between the two sets of estimates. Additional Monte Carlo sensitivity tests, in which each input parameter was perturbed individually***

while the others were held constant, showed that uncertainties in V_{PM} and κ_{rPM} contributed most strongly to the uncertainty in the retrieved κ_{OA} (Fig. S15c).”

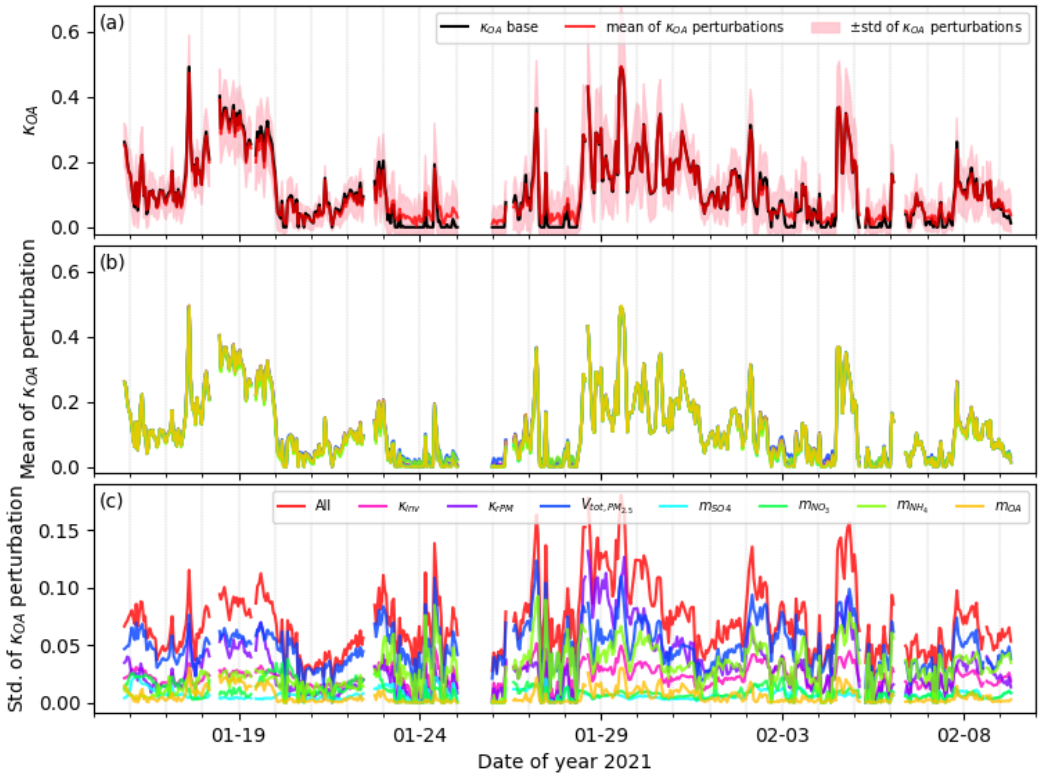

Figure R2-1. Time series of (a) Monte Carlo mean values of κ_{OA} (red line) and the ±1 standard deviation range around the Monte Carlo mean (light red shading), compared with the baseline estimates (black line); (b) Monte Carlo mean values of κ_{OA} obtained by perturbing individual input parameters including κ_{inv}, the mass concentrations of non-refractory species, the total particle volume concentration, and κ_{rPM}; and (c) the corresponding standard deviations of κ_{OA} for each individual perturbation..

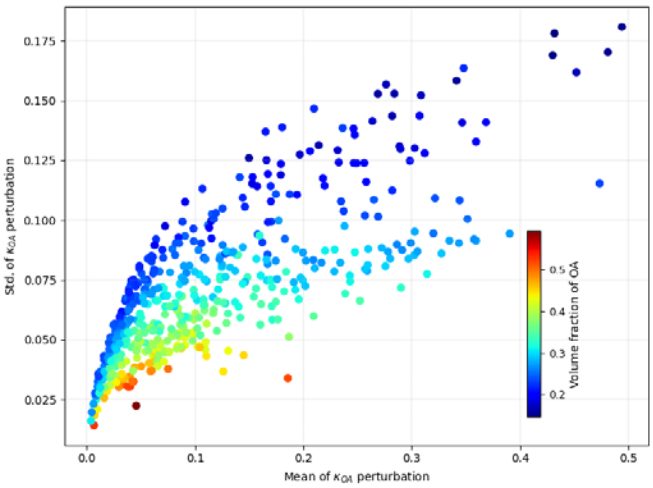

Figure R2-2. Monte Carlo standard deviations of κ_{OA} as a function of the corresponding Monte Carlo mean values, colored by the volume fraction of OA in $PM_{2.5}$.

2. Line 175 – 185: The relative contribution of biomass burning to BC f_{bb} is derived assuming fixed AAE values of 1.0 and 2.0 for fossil-fuel and biomass-burning emissions, respectively. I suggest the authors discuss this uncertainty using fixed AAE.

Response: We thank the reviewer for this helpful suggestion. We acknowledge that estimating the relative contribution of biomass burning to BC (f_{bb}) using fixed absorption Ångström exponent (AAE) values of 1.0 and 2.0 for fossil-fuel and biomass-burning emissions, respectively, introduces uncertainty into the estimated f_{bb} values. However, the primary objective of this study is to investigate the factors influencing ambient κ_{OA}, rather than to obtain an exact estimate of f_{bb}. Therefore, we conducted a sensitivity analysis to assess whether the κ_{OA}-f_{bb} relationship is sensitive to the assumed AAE values.

First, we varied the AAE for biomass-burning emissions (AAE_{bb}) while keeping the fossil-fuel AAE (AAE_{ff}) fixed at 1.0. Compared with the baseline case of AAE_{bb}=2.0, using a lower value of 1.8 resulted in higher estimated f_{bb} values, whereas using a higher value of 2.2 resulted in lower estimates. Nevertheless, the increasing trend of κ_{OA} with increasing f_{bb} remained unchanged. We also varied AAE_{ff} by ±10% around the baseline value of 1.0 while keeping AAE_{bb}=2.0. The resulting κ_{OA}-f_{bb} relationships remained qualitatively consistent, although the absolute f_{bb} values varied with the assumed AAE parameters.

These sensitivity tests suggest that, although the absolute estimates of f_{bb} depend on the assumed AAE values, the main increasing relationship between κ_{OA} and f_{bb} is qualitatively robust to the tested variations in AAE. We have added this sensitivity analysis and the associated discussion to the revised manuscript.

Section 3.4, lines 416-419: "***The robustness of the κ_{OA}-f_{bb} relationship was examined through sensitivity tests by varying AAE_{bb} from 2.0 to 1.8 and 2.2 while keeping AAE_{ff} fixed at 1.0, and by varying AAE_{ff} from 1.0 to 0.9 and 1.1 while keeping AAE_{bb} fixed at 2.0. Although the estimated f_{bb} values varied with the assumed AAE parameters, the increasing trend of κ_{OA} with f_{bb} remained qualitatively consistent (Fig. S17).***"

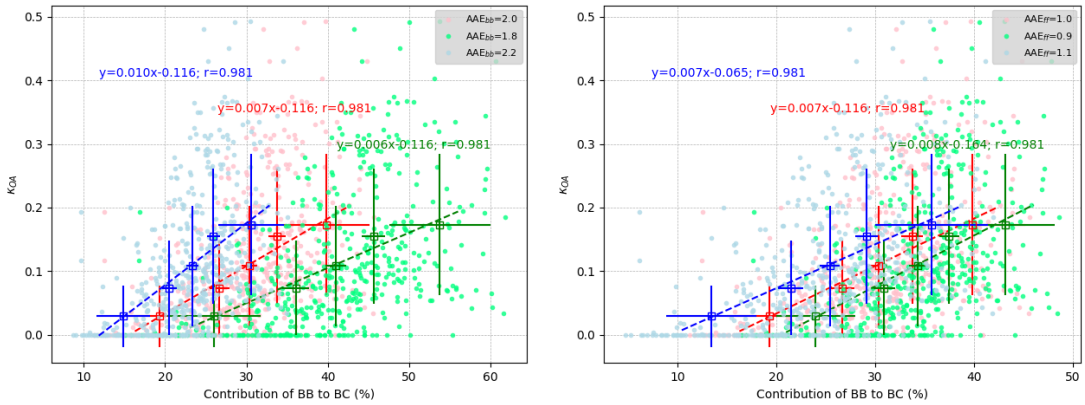

Figure R2-3. Variation of κ_{OA} as a function of relative contribution of biomass burning to BC (f_{bb}) under different assumptions for the absorption Ångström exponents (AAEs). Open squares represent binned mean κ_{OA} values based on f_{bb} bins defined by 20th-percentile intervals, with error bars indicating one standard deviation. Dashed line shows a linear regression fitted to the binned means. The left panel shows the κ_{OA}-f_{bb} relationships obtained by fixing fossil-fuel AAE (AAE_{ff}) at 1.0 and varying biomass-burning AAE (AAE_{bb}) among 1.8 (green), 2.0 (red) and 2.2 (blue). The right panel shows the relationships obtained by fixing AAE_{bb} at 2.0 and varying while AAE_{ff} varying among 0.9 (green), 1.0 (red) and 1.1 (blue).

3. Line 313–319: The authors show that κ_{inv} systematically decreases with increasing RH. While in Line 239–242, the κ_{inv} retrieved over 80–90% RH is used to represent bulk aerosol hygroscopicity and derive κ_{OA}. Given the observed RH dependence of κ_{inv}, I suggest the authors to assess whether the choice of RH interval affects the derived κ_{OA} and its main relationships with source and oxidation indicators.

Response: We thank the reviewer for this helpful suggestion. As discussed in Section 3.2 of the manuscript, the retrieved hygroscopicity parameter (κ) exhibited a systematic decrease with increasing RH. This RH dependence may reflect non-ideal solution thermodynamics, changes in solute mass fractions, liquid-liquid phase separation, and other factors. Nevertheless, we use κ_{inv} retrieved over the 80-90% RH range as the representative value in the main analysis because this RH interval is commonly used in previous studies employing humidified tandem differential mobility analyzers (H-TDMAs; Wu et al., 2016; Hong et al., 2018) and humidified nephelometer systems (Kuang et al., 2020; Titos et al., 2021), facilitating comparison with previous results.

Because the component-specific hygroscopicity parameters adopted for ammonium nitrate (AN), ammonium sulfate (AS), ammonium bisulfate (ABS), and particulate chloride (PC) in the Zdanovskii-Stokes-Robinson (ZSR) mixing rule are representative of approximately 85% RH, the κ_{OA} values derived in the main analysis should likewise

be interpreted as representative of this RH condition. To assess the sensitivity of the derived κ_{OA} to the choice of RH interval, we additionally estimated κ_{OA} at approximately 65% and 75% RH.

Zhao et al. (2022) reported that the hygroscopicity parameter of AS decreases from approximately 0.73 at 60% RH to 0.42 at 95% RH, corresponding to an average decrease of approximately 0.009 per percentage point of RH. In the absence of comparable RH-dependent parameterizations for the other inorganic components considered in this study, we used this decrease rate as a first-order approximation to adjust their hygroscopicity parameters to lower RH conditions. We then applied the ZSR mixing rule using the bulk κ values retrieved over the 60-70% RH interval and the adjusted inorganic-component parameters to estimate κ_{OA} at approximately 65% RH. The same procedure was applied to estimate κ_{OA} at approximately 75% RH using the bulk κ values retrieved over the 70-80% RH interval. We acknowledge that this approximation introduces additional uncertainty into the lower-RH estimates.

As shown in Figure R2-4, the κ_{OA} estimates exhibit similar temporal variations across the RH intervals, with correlation coefficients of 0.71 and 0.90 between the estimates at approximately 65% and 75% RH, respectively, and those at approximately 85% RH. In particular, the κ_{OA}–f_{bb} relationships at 75% and 85% RH exhibit similar increasing trends, although the estimated κ_{OA} values are systematically higher at 75% RH (Figure R2-5). These results suggest that the qualitative relationship between κ_{OA} and biomass-burning contribution is relatively robust to the choice of RH interval, despite some RH-dependent differences in the absolute κ_{OA} values. Nevertheless, given the additional uncertainty associated with the insufficiently characterized RH dependence of the inorganic components, we retain the κ_{OA} estimates representative of approximately 85% RH for the main analysis. We have clarified the rationale for selecting the 80–90% RH interval in the revised manuscript.

Section 2.3.2, lines 242-245: “Unless otherwise specified, κ_{inv} values retrieved over the 80–90% RH range are used to represent bulk aerosol hygroscopicity, as the results are directly comparable ***with*** previous studies that report κ_{inv} within this RH range (Kuang et al., 2020; 2021) ***and are consistent with the RH conditions corresponding to the κ values adopted for well-characterized inorganic species when estimating OA hygroscopicity, as discussed below***.”

Section 2.3.3, lines 273-275: “***Since κ is RH dependent under sub-saturation conditions (Zhao et al., 2022), the selected values are assumed to represent aerosol hygroscopicity at an RH of ~85%, consistent with the κ_{inv} values retrieved over the 80–90% RH range.***”

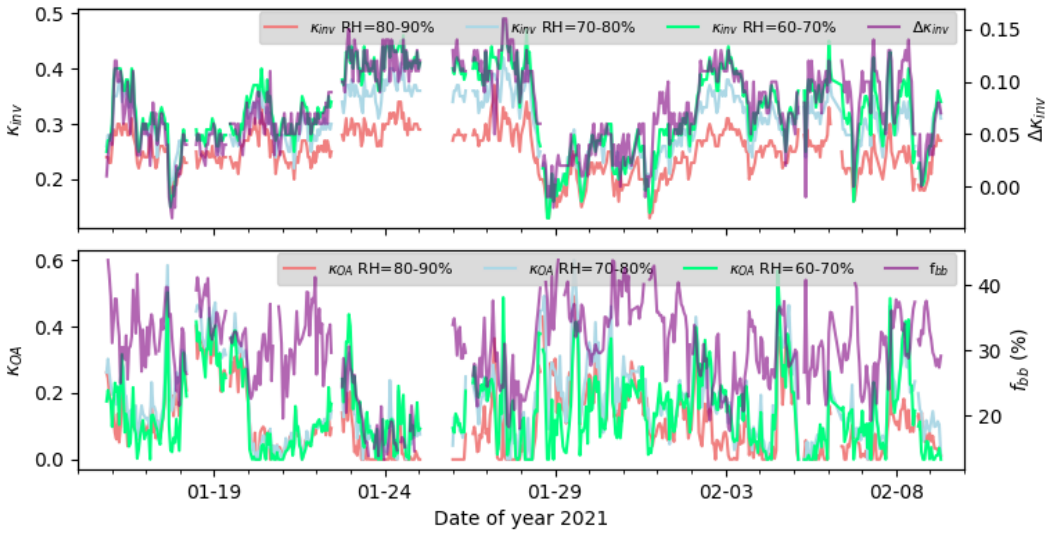

Figure R2-4. Bulk κ retrieved for RH intervals of 80–90% (red), 70–80% (blue), and 60–70% (green), along with the difference between κ at 80–90% and 60–70% RH (purple) in the upper panel. The lower panel shows the corresponding κ values of OA for the three RH intervals and the biomass-burning contribution.

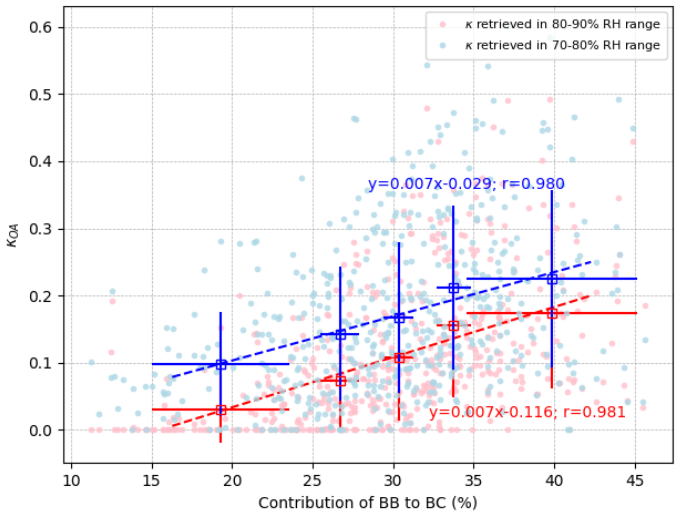

Figure R2-5. Variation of κ_{OA} retrieved for RH intervals of 80-90% (red) and 70-80% (blue) as a function of relative contribution of biomass burning to BC (f_{bb}). Open squares represent binned mean κ_{OA} values based on f_{bb} bins defined by 20th-percentile intervals, with error bars indicating one standard deviation. The dashed line shows a linear regression fitted to the binned means.

4. Line 218–219 and 234–235: The Mie calculation of $B_{sp,dry}$ accounts for the angular response of the Aurora 3000 nephelometer. Please clarify whether the angular response of the Aurora 1000 nephelometer was similarly considered when calculating $B_{sp,wet}$.

Response: We thank the reviewer for this insightful comment. The angular response correction was considered in the calculations of both the dry and wet scattering coefficients ($B_{sp,dry}$ and $B_{sp,wet}$ respectively).

Specifically, the angular sensitivity function, Z(θ), was derived following the equations (Eq. 10) and parameter values (Table 2) reported by Müller et al. (2011) for the Aurora 3000 nephelometer. Although the corresponding parameters for the Aurora 1000 are not available in Müller et al. (2011), we assumed that the same angular sensitivity parameters could be applied to the Aurora 1000 because the two nephelometers share the same manufacturer and a similar instrument design. We acknowledge that this assumption is based on their design similarity rather than an independent characterization of the Aurora 1000 angular response.

The resulting angular sensitivity function, Z(θ), was incorporated into the Mie calculations in place of the ideal angular weighting function, sin(θ), to calculate the scattering efficiency (Q) as a function of particle size. Figure R2-6 compares the scattering efficiencies calculated using the ideal and non-ideal angular weighting functions. The results show that accounting for the nephelometer's angular response yields generally lower scattering efficiencies across the particle sizes considered. These non-ideal scattering efficiencies were then combined with the particle number size distribution (PNSD) to calculate the scattering coefficients for both dry and wet aerosols.

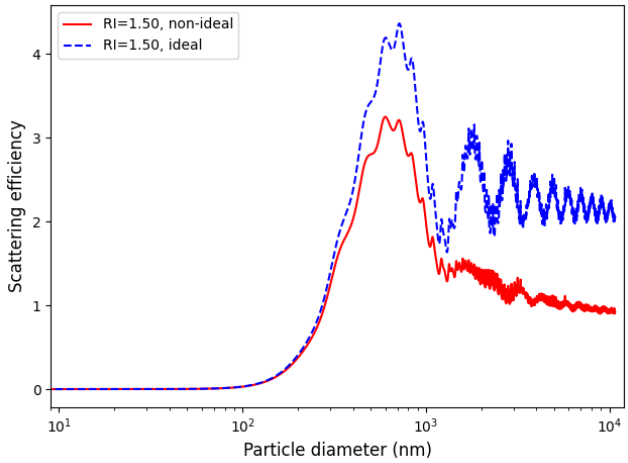

Figure R2-6. Comparison of scattering efficiencies calculated using Mie theory with a non-ideal angular weighting function (i.e., the angular sensitivity function; red solid line) and an ideal angular weighting function (sin(θ); blue dashed line). The calculations were performed at an incident wavelength of 520 nm and a particle refractive index of $1.50+10^{-7}$i.

To improve computational efficiency, we precomputed the non-ideal scattering efficiencies and constructed a lookup table as a function of the refractive index (RI) and

particle size parameter ($x=\pi d/\lambda$, where d is the particle diameter and λ is the wavelength of incident light). This approach was applied consistently to both the dry and wet aerosol calculations.

In the revised manuscript, we have clarified that the angular response correction was also considered when calculating $B_{sp,wet}$.

Section 2.3.2, lines 235-237: "***Notably, the angular response correction was also applied in calculating $B_{sp,wet,calc}$, assuming that the Aurora 1000 shares the same angular sensitivity function as the Aurora 3000, as reported by Müller et al. (2011), owing to their similar instrument designs.***"

5. Line 245: "a simply proxy" should be "a simple proxy".

Response: Thank you for pointing this out. We have corrected the wording accordingly.

6. Line 270: "The consistent between..." should be "The consistency between...".

Response: Thank you for pointing this out. We have corrected the wording accordingly.

7. Figure 5 caption: "20% percentiles" should be "20-percentile intervals".

Response: Thanks for this comment. We have revised the caption of Figure 5 accordingly.

8. Figure 3: The legend for O:C and fbb is unclear. Please revise it to improve readability.

Response: Thank you for this helpful suggestion. We have revised the legend in Figure 3 to improve its clarity and readability.

References:

Hong, J., Xu, H. B., Tan, H. B., et al.: Mixing state and particle hygroscopicity of organic-dominated aerosols over the Pearl River Delta region in China, Atmos. Chem. Phys., 18, 14079–14094, https://doi.org/10.5194/acp-18-14079-2018, 2018.

Kuang, Y., He, Y., Xu, W. Y., et al.: Distinct diurnal variation in organic aerosol hygroscopicity and its relationship with oxygenated organic aerosol, Atmos. Chem.

Phys., 20(2), 865–880, https://doi.org/10.5194/acp-20-865-2020, 2020.

Müller, T., Laborde, M., Kassell, G., and Wiedensohler, A.: Design and performance of a three-wavelength LED-based total scatter and backscatter integrating nephelometer, Atmos. Meas. Tech., 4(6), 1291–1303, https://doi.org/10.5194/amt-4-1291-2011, 2011.

Titos, G. Burgos, M. A., Zieger, P., et al.: A global study of hygroscopicity-driven light-scattering enhancement in the context of other in situ aerosol optical properties, Atmos. Chem. Phys., 21, 13031–13050, https://doi.org/10.5194/acp-21-13031-2021, 2021.

Wu, Z. J., Zheng, J., Shang, D. J., et al.: Particle hygroscopicity and its link to chemical composition in the urban atmosphere of Beijing, China, during summertime, Atmos. Chem. Phys., 16, 1123–1138, https://doi.org/10.5194/acp-16-1123-2016, 2016.